



Retinal Image Contrast Enhancement through Pixel Collaboration in Spatial Domain

Yeddu Aruna Suhasini Devi^{1*} Manjunatha Chari Kamsali²

¹*Department, of Electronics and Communication Engineering,
CMR College of Engineering, Hyderabad, Telangana, India*

²*Department, of Electrical Electronics and Communication Engineering,
GITAM University, Hyderabad, Telangana, India*

* Corresponding author's Email: arunasuha@gmail.com

Abstract: Retinal images have a significant role in the diagnosis of Diabetic Retinopathy. However, the main objects of retinal images are Retinal Vessels, Exudates, and Microaneurysms which are of low contrast. Hence, this paper proposes a new contrast enhancement mechanism called as Spatial Collaborative Contrast Enhancement (SCCE). SCCE utilizes the mutual relation and spatial spread of gray levels over the retinal image and enhances the contrast. SCCE allocates one rank for every pair of gray levels and ensures a perfect gap between consecutive gray levels that result in an increased contrast in the output retinal image. Several experiments are performed on two standard datasets namely HRF and DRIVE. Experimental results show that the proposed SCCE method improves the contrast of retinal images in a better manner than several existing methods including CLAHE and Normalized Convolution (NC). On an average, the SCCE gained an improvement of 14% and 3% in SSIM from CLAHE and NC respectively.

Keywords: Retinal images, Contrast enhancement, Histogram, Histogram equalization, Mutual dependency, Contrast improvement index.

1. Introduction

From the past few years, in almost all parts of the world, a gradual increase has been observed in retinal diseases (ex. Diabetic retinopathy, macular degeneration, glaucoma etc.) in the aged and working population. Among different kinds of retinal diseases, Diabetic Retinopathy (DR) is one of the most chronic diseases which may consequence to permanent blindness, particularly for the middle aged people. According to several studies [1, 2], it was predicted that the people affected with DR will rise from 126.6 million in 2011 to approximately 191 million by the end of year 2030. In India, this number is approximated as very high and it was found that the DR is sixth biggest cause of vision loss. This number is further approximated to grow enormously due to the rise of diabetic patients. The better solution to control this growth is a speedy and accurate diagnosis of DR through retinal images.

The blood vascular structure of a retinal image has a major role in the diagnosis of DR. Doctors or radiologists can determine the DR stage just by observing the blood vessel's structure. For instance, the initial stage of DR is determined if the retinal image is found to have tiny bulges and high tortuosity of the blood vessels. On the other hand, the advanced stage of DR can be determined with the presence of larger number of tiny blood vessels branching out from major blood vessels. The initial stage of DR is termed as Non-proliferative DR (NPDR) while the advanced stage is termed as proliferate DR (PDR) [3] and it is the main reason for vision loss in individuals.

To analyze the blood vascular structure in retina images, the vessels need to be segmented from retinal image. For an accurate segmentation of the blood vessels from retinal image, the quality of retinal image must be high. However, acquiring such kind of qualitative images is not possible due to

several reasons like distance between retina and imaging device, eye ball's movement and eyelid's improper expansion etc. Some more reasons include diseases like cataract, unnecessary movements of patient's eye, dilation degree and retina's curved surface [4]. Except the first reason, the remaining reasons result in a low contrast and improperly illuminated retinal image while the first reason results in a blurry retinal image. Since the cataract prevents the light from reaching the retina, it produces a less qualitative blurry retinal image. Due to these reasons, the retinal images suffer from low contrast and non-uniform illumination problems. Considering such kind of low quality images results in an inaccurate diagnosis, because they can't support accurate segmentation of vessel structure. Hence, there is a need for pre-processing phase which involves the task of contrast and illumination adjustment in low qualitative retinal images before subjecting them for segmentation.

The main aim of this paper is to address the problem of uneven contrast in retinal images that happens during the image acquisition. This paper concentrates on the pre-processing phase that deals with enhancement of image quality in terms of contrast. This phase has an important role in the accurate segmentation of blood vascular structure followed by accurate diagnosis of DR. Towards such objective this paper proposes a new contrast enhancement method called as Spatial Collaborative Contrast Enhancement (SCCE) which computes the collaboration between consecutive gray levels such that they can be separated effectively in output image. For spatial collaboration, we measured the 2D spatial joint histogram followed by mutual information between two gray levels. Based on the obtained values, a rank is assigned and used in the newly derived mapping function.

Rest of the paper is structured as follows: the details of literature survey on contrast enhancement methods for retinal images are explored in Section 2. Section 3 reveals the details of proposed methodology of contrast enhancement. Section 4 reveals the details of experiments and Section 5 concludes the paper.

2. Literature survey

For an accurate diagnosis of DR, the input retinal image must be more qualitative and it must be free from several constraints like lower contrast, uneven illuminations etc. To meet these requirements, the retinal images must be pre-processed. Hence, different researchers developed different methods and tried to improve the quality of

retinal image. Contrast enhancement (CE) is a widely studied technique in retinal images which is employed to ensure a perfect discrimination between vessels and background and improves the quality of image [5].

In general, with respect to the methodology followed for CE, the earlier developed CE methods are classified into two categories; they are Local Contrast Enhancement (LCE) and Global Contrast Enhancement (GCE) methods [6]. In GCE, the global information of retinal image is used for CE while in the LCE, local information is employed. LCE methods generally apply windowing techniques to split the image into local blocks and the CE is done in each and every block. Further, some methods applied both GCE and LCE and they are called as hybrid methods. In these methods, the retinal image is initially processed for GCE and then different methods like Short Time Fourier Transform (STFT), Discrete cosine transform (DCT) etc., are applied for LCE. However, both have advantages and disadvantages and they are explored through state-of-the-art methods here.

Histogram Equalization (HE) [7, 8] is one of the most commonly used method that was employed by most of researchers in the CE of retinal images. HE performs a mapping operation between input and output images by deriving a matching function through the Cumulative Distributive Function (CDF) of input retinal image. However, HE doesn't preserve the Mean Brightness of Image (MBI).

In Global Histogram Equalization (GHE) [9], the entire range of gray-scale pixel intensities is considered for equalization. However, GHE introduces over enhancement, especially for the larger peaks in the histogram. Due to this reason, the output images suffer from harsh and noise components.

To overcome these problems, Adaptive Histogram Equalization (AHE) [10] methods are developed in which the CE is done locally by considering the local pixel's intensities. However, AHE methods amplify the noise along with contrast of pixel surrounded by local pixels. To solve this problem, a new version of AHE called as "Contrast Limited Adaptive Histogram Equalization (CLAHE)" [11-13] was introduced which keeps a threshold limit such that the retinal image is protected from over enhancement. With an inspiration of CLAHE, J. Thani et al. [14] applied it to preserve the color information of retinal images. They proposed an Improved Non-linear Hue-Saturation-intensity color model (INHSI) in which the intensity component is enhanced by Rayleigh Transformation in CLAHE. Though CLAHE has shown an effective

performance in CE, it can't support for full-fledged MBI preservation. Moreover, the CLAHE also introduces ringing artifacts at edges and also amplifies the noises in the smoother regions. Moreover, the CLAHE needs an appropriate parameter setting for each individual gray level. The parameter fixed for one level won't contribute much for the other level or other images. Compared to HE, CLAHE had shown better performance, however, fixing a proper threshold limit is tough task.

Some more approaches are developed for the retinal image CE. Rampal et al., [15] employed a new filter called "Complex Diffusion-Based Shock Filter (CDSF)" for smoothing and CE of retinal images. CDSF is a non-linear forward-backward diffusion based filter developed by Gilboa et al. [16] with an aim for image enhancement by removing speckle noises, compression artifacts reduction in JPEG and for an adaptive CE. CDSF is more sensitive to color artifacts in retinal images.

Liao et al., [17] employed an integrated CE model by combining the Histogram Fitting Stretching (HFS) and Multi-scale Top-hat Transform (MSTT). Initially, the optimal bright and dim features are extracted through MSTT [18] and then the image is enhanced by removing dim features and adding bright features. Finally, the initially enhanced image is processed through HFS [19] for further enhancement. Though this hybrid model attained an effective quality, it has introduced some external artifacts like spontaneous variations in the color levels, artificial boundaries, and loss of information in retinal images.

To resolve this problem, Fan. M. et al. [20] proposed a new CE method based on normalized convolution. This approach removes noise in the image with the help of "Partial Differential Equations (PDE)" and enhances contrast with "Relaxed Median Filter (RMF)". First, the image is transformed through normalized convolution algorithm [21] to extract the basic background information. Then the image is fused with original image to obtain an enhanced retinal image. Finally, the fused image is subjected to denoising through a two stage process composed of PDEs and RMF. However, PDEs can't identify the pixels with noise components. Moreover, the RMF is best method for filtering noise but not for contrast enhancement.

Next, L. Luo et al. [22] employed sparse-coding and multi-dictionary coding for retinal image enhancement. Two distinct dictionaries are developed namely, "Enhanced Dictionary (ED)" and "Representation Dictionary (RD)". The information in multi-dictionary is optimized based on the patches extracted through RD. RD is generated from original

retinal images and ED is generated from the corresponding label images. CE through dictionary based sparse coding introduced the computational complexity as it follows an iterative process and at each iteration, the previous resultant is compared with previous output.

Xu. Liang and Li. Xiong [23] focused on the enhancement of retinal image's quality and adopted for scattering based image formation model. Initially, they estimated the foreground and background with the help of Global Spatial Entropy and Mahalanobis distance from low and high intensity region respectively. Due to this estimation, this method performed well for blurry images. Global entropy introduces ringing artifacts in retinal images.

M. Zhou et al. [24] proposed a CE algorithm based on a luminance gain matrix that was obtained by gamma correction of the value channel in HSV (Hue-Saturation-Value) color space. The luminance gain matrix is used to enhance R, G and B channels respectively. Contrast is then enhanced in the luminosity channel of L^*a^*b color space by CLAHE. Enhancement in HSV domain introduces spontaneous blur in the enhanced image.

Sima Sahu et al. [25] employed the same CLAHE algorithm for CE and noise removal in retinal images. This method employed different set of filters along with CLAHE for CE in retinal images. Different set of filters namely median filter, wiener filter, Gaussian filter, weighted median filter and Average filter are employed for denoising. However, they were not aimed at the enhancement of contrast enhancement of green channel which has more significant information.

Gupta, B. Tiwari, M. [26] proposed an overall CE method for retinal images. Initially, they calculated a gain matrix with the help of luminance values which were obtained by adaptive gamma correction method and it was used to enhance all the three color channels of retinal images. Afterwards, Quintile based HE is employed to enhance the overall visibility of images. A. A. Bala et al. [27] proposed Multi-resolution curvelet transform (CT) and adaptive sigmoid mapping of Histogram Equalization for CE in retinal images. Initially, they decomposed the retinal image into several sub bands through CT and then applied hard thresholding over each coefficient to remove the noise. CT removes the spatial correlation between pixels of images and the reconstruction results in spurious holes.

Even though the above mentioned methods achieved an efficient performance in the retinal image enhancement, they didn't perform contrast enhancement based on the level of contrast available on an image. This kind of enhancement results in

degraded contrast in the case of image with high level of contrast. Moreover, the CE is generally used as pre-processing step; hence the algorithm must be able to provide better results with its default parameters. Most of the above methods defined new parameters and they tried to optimize them. Such kind of enhancement performs well only for some types of images and does not work well on the images with much degradation in quality.

3. Proposed approach

3.1 Overview

In this paper, we propose a new contrast enhancement method called as Spatial Collaborative Contrast Enhancement (SCCE) to enhance the quality of retinal images. The main intention behind this method is to make the retinal images more qualitative such that the features (like vessels, optic disk, exudates etc.) visualize better and helps in the accurate diagnosis of Diabetic Retinopathy. This approach defined a new definition for mutual dependency between gray levels of the retinal image. The proposed method tends to utilize the complete dynamic range of image gray-levels during CE. This approach quantifies the mutual dependency between gray levels according to their spatial spread over the image and dependency. The new definition of Mutual dependency allows calculating the joint spatial statistics in a computationally efficient manner. For a given low contrast retinal input image, the proposed method maps its gray levels to the optimal gray levels such that the perceived contrast of output images is better. Figure.1 shows the simple schematic of proposed contrast enhancement mechanism.

3.2 Spatial entropy based CE (SECE)

SECE is a global contrast enhancement method which aims at the creation of a naturally looking

image with an appropriate contrast level at all portions of image [28]. SECE utilizes the entire dynamic range, i.e., 0-255 of an eight bit retina image. SECE initially finds the 2D spatial histograms of all distinct gray levels by placing a spatial grid over the input image. The spatial grid size is selected in such a way that the aspect ratio of input image and spatial grid must be nearly equal. Once the size of spatial grid is determined, then it slides over the input image along both rows and columns. For every slide, the SECE finds 2D spatial histograms of each and every gray level. After the determination of 2D histograms they are processed for entropy calculation followed by Cumulative Distribution Function (CDF) calculation. Based on the obtained CDF value, the input image is mapped to output image through the dynamic range of gray levels.

Consider an input retinal image A of size $P \times Q$, where P denotes the total number of rows and Q denotes the total number of columns. Based on these dimensions, the image A is represented as $A = \{a(i, j) | 0 \leq i \leq P - 1, 0 \leq j \leq Q - 1\}$. Assume that the input retinal image A has a dynamic range of gray level intensities that lies between the lower limit a_l and the upper limit a_u , then the image pixel is denoted as $a(i, j) \in [a_l, a_u]$. Next, consider B to be the output image or contrast enhanced image which can also be represented like image A , as $B = \{b(i, j) | 0 \leq i \leq P - 1, 0 \leq j \leq Q - 1\}$. Let the dynamic range of B be denoted as b_l and b_u , where the former denotes the lower limit and the latter denotes upper limit of gray level intensities in contrast enhanced image. So every pixel of image B lies within the upper and lower limits of range and hence it can be denoted as $b(i, j) \in [b_l, b_u]$. To obtain an optimal contrast in the output image, this work is supposed to use the entire dynamic range, i.e., 0 to 255 for an 8-bit image. Moreover, the

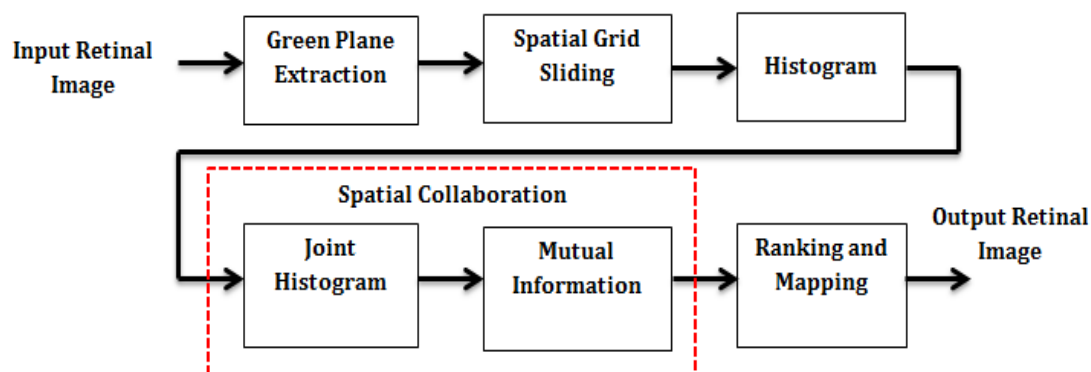


Figure. 1 Block diagram of proposed SCCE

SECE also assumed that lower limit is always less than the upper limit, i.e., $b_l < b_u$] and $b_l = 0$ and $b_u = 2^8 - 1 = 255$ for an 8-bit image.

3.2.1. Spatial histogram

A 2D spatial histogram is defined as the total number of occurrences of a gray level in 2D image or region. In SECE, instead of considering the entire image as one region, it was initially divided into several small regions with the help of a spatial grid. So, the first aspect is to determine the size of spatial grid. For this purpose, SECE considered two parameters. They are Eq. (2) Size of input retinal image and Eq. (1) Aspect ratio (r). The aspect ratio is measured based on the row size and column size of input image, as

$$r = \frac{P}{Q} \quad (1)$$

Now, the size of spatial grid is measured with the help of r and size of input image. Consider T to be the row size of spatial grid and S to be the column size of spatial grid, they are measured as follows;

$$T = \left\lceil \sqrt{\left(\frac{G}{r}\right)} \right\rceil \text{ and } S = \left\lceil \sqrt{(G \times r)} \right\rceil \quad (2)$$

Where G is the total number of distinct gray levels present in the input retinal image and $\lceil \cdot \rceil$ represents the ceil operation which rounds off the obtained value to its nearest integer. Based on these two size factors, the total number of grids into which the image can be divided is calculated as $T \times S$. Now define two iterating variables t and s , where $1 \leq t \leq T$ and $1 \leq s \leq S$. These two variables help the spatial grid to slide over the input image. The input image region on which the spatial grid needs to be located is measured as

$$\left[(t-1) \frac{P}{T}, t \frac{P}{T} \right] \times \left[(s-1) \frac{Q}{S}, s \frac{Q}{S} \right] \quad (3)$$

According to the above expression, there is a possibility of obtaining total $T \times S$ number of regions. For every image region, the 2D spatial histogram is measured for all gray levels. Consider there exists G number of distinct gray levels in input image and let them be denoted as $\{a_1, a_2, \dots, a_G\}$, where $\{a_1 < a_2 < \dots < a_G\}$ after sorting them. Similarly, the gray levels of output images be denoted as $\{b_1, b_2, \dots, b_G\}$, where $\{b_1 < b_2 < \dots < b_G\}$ after sorting them. For instance, the 2D spatial

histogram of a gray level a_g on the spatial grid located on the image region is calculated as

$$h_g = \{h_g(t, s) | 1 \leq t \leq T \text{ and } 1 \leq s \leq S\} \quad (4)$$

Where t and s are two real numbers and $h_g(t, s)$ denotes the total number of occurrences of the gray level a_g on the specified spatial grid. Here an important point to notice is, the aspect ratio of spatial grid must be approximately equal to the aspect ratio of original input image, i.e., $r = \frac{P}{Q} \approx \frac{T}{S}$.

3.2.2. Entropy and mapping

Once the computation of each gray level on different spatial grids is completed, then SECE calculates the entropy of each level with the help of histograms $h_{g,g=1,2,\dots,G}$. Consider the entropy of g^{th} gray level a_g as E_g and it is obtained as

$$E_g = - \sum_{t=1}^T \sum_{s=1}^S h_g(t, s) \log_2(h_g(t, s)) \quad (5)$$

Next, SECE computes the relation between their entropies, as

$$f_g = E_g / \sum_{l=1, l \neq g}^G E_l \quad (6)$$

The obtained discrete function f_g measures the relative importance of gray level a_g with other gray levels $a_l, l \neq g$ and l varies from 1 to G. For larger values of f_g , the relative importance is said to be high and vice versa. A larger value of h_g determines the larger number of occurrences of the corresponding gray level a_g . Next, based on the obtained discrete function f_g , the cumulative distribution function is calculated as

$$F_g = \sum_{l=1}^g f_l \quad (7)$$

where F_g is the CDF of a gray level a_g and it is used to map a_g to b_g with the help of upper and lower limits of output image. The mapping is done according to the following expression;

$$b_g = \lceil F_g(b_u - b_l) + b_l \rceil \quad (8)$$

3.3 SCCE

SECE method performs the global contrast enhancement by mapping the gray levels of input image to the gray levels of output image. The mapping is done with the help of a weight vector

computed, based on the spatial entropy of gray levels. For a particular gray level, its weight is calculated as a ratio of the spatial entropy of corresponding gray level to the summation of spatial entropies of remaining gray levels. This process is also called as a normalization process which shows the relative importance of a gray level with other gray levels. Due to this process, SECE has gained a slight improvement in the global contrast. Moreover, the SECE doesn't consider the spatial relationship between gray levels, thus most of the time, the gray level of an output image is linear function of gray level of input image. Due to the process of histogram specification and mean brightness preservation, the SECE is not able to utilize the complete dynamic range which may result in the loss of contrast in the output image.

To overcome these problems of SECE, this paper proposed a new method called as Spatial Collaborative Contrast Enhancement (SCCE or SC²E). SCCE computes the weight between two gray levels with respect to their dependence and the spatial spread over the image. Spatial Collaboration (SC) quantifies the spatial distribution and proximity of the two gray levels over the image. For every SC, a rank is assigned and it is used to provide a larger gap between consecutive gray levels. For the two gray levels with high SC, the proposed method allocates larger gap such that the perceived contrast is high in the output image.

3.3.1. Spatial collaboration

Consider two gray levels of the input image as a_g and a_k and the corresponding histograms are denoted as $h_g(t, s)$ and $h_k(t, s)$ respectively. The spatial relationship between these two gray levels is computed through 2D spatial joint histogram which can be denoted as $h_{g,k}(t, s)$. The term $h_{g,k}(t, s)$ represents the occurrence of two gray levels on an image region as obtained through Eq. (3). $h_{g,k}(t, s)$ and is calculated as

$$h_{g,k}(t, s) = \text{average}(h_g(t, s), h_k(t, s)) \quad (9)$$

This new definition of 2D spatial joint histogram denotes the proportion of occurrence of gray levels a_g and a_k on the specified image region. $h_{g,k}(t, s)$ helps to calculate the joint spatial statistics of two gray levels in a computationally efficient manner. Based on the obtained 2D joint spatial histogram, we can determine the mutual dependency and spatial spread of two gray levels over the image. For the assessment of spatial collaboration between different

gray levels in the image, we referred the mutual information which is denoted as $I_{g,k}$ and it is calculated as follows [29]

$$I_{g,k} = \sum_{t=1}^T \sum_{s=1}^S h_{g,k}(t, s) \log_2 \left(\frac{h_{g,k}(t, s)}{h_g(t, s)h_k(t, s)} \right) \quad (10)$$

Where $h_{g,k}(t, s)$ is obtained through Eq. (9) and $h_g(t, s)$ or $h_k(t, s)$ are obtained through Eq. (4). Based on the obtained mutual information, we can determine the mutual dependency between two gray levels a_g and a_k . If the obtained mutual information $I_{g,k}$ is high, then it can be denoted that they occur jointly on close spatial regions and spread over the image region. Hence we can allocate the larger gaps between the output gray levels b_g and b_k such that the contrast of output image is better than the input image.

3.3.2. Rankling and mapping

The SC between two gray levels a_g and a_k can be used to compute the mutual dependency of the gray level a_g and on the other gray levels $a_{k,k=1,2,\dots,G}$. Hence, it forms a two dimensional symmetric matrix that represents the dependencies between pair-wise gray levels. Such kind of matrix is used to allocate a rank for every gray level according to its relation with other gray levels. For instance, consider the image having ten distinct gray levels, then the matrix is derived based on their SC's and it is of size 10×10 . The first row denotes the SC between first gray level with remaining gray levels. Next, the second row denotes the SC of second gray level with remaining gray levels. Finally the last row denotes the SC of last gray level with reminding gray levels. This matrix is also called as hyperlink matrix which has same number of rows and columns.

Consider $Z = \{z(g, k) | 0 \leq g \leq G - 1, 0 \leq k \leq G - 1\}$ be a $G \times G$ hyperlink matrix where G represents the total number of Gray levels present in the image, $z(g, k)$ represents the SC between two gray levels a_g and a_k where it can be simply replaced with the Mutual information $I_{g,k}$. The SC between two gray levels is said to be high if they have uniform distribution on spatial domain image and their occurrence is on the same spatial grid. In the image, due to larger correlation between pixels, the occurrence of adjacent gray levels is much high. It means the SC between adjacent gray levels is high. For a given row (gray level) in hyperlink matrix, only few columns are occupied with lager values while most

of the columns are zeros. So, for each gray level a_g , there exists at least one gray level a_k for which $z(g, k) \neq 0$. Based on this hyperlink matrix, the rank is calculated as [30]

$$r(g, k) = \frac{z(g, k)}{\sum_{k=1}^G z(g, k)} \quad (11)$$

Where $r(g, k)$ is the rank assigned based on the SC between two gray levels and it signifies dependency and spatial spread of two gray levels in the spatial domain of input image. Based on this rank information, a new mapping function is derived to map the gray levels of input image to the gray levels of output image. The newly defined mapping function is represented as

$$b_g = \lfloor b_{g-1} + \Omega_{g-1, g}(b_u - b_l) \rfloor \quad (12)$$

The above expression denotes that the gray level at g is dependent on the gray level at $g-1$ and also on the gap between the gray levels at g and $g-1$. Moreover, the above equations start from $g=2$ and for $g=1$, $b_1 = b_l$, it means that the initial gray level in the output image is nothing but the lower limit. Next, the term $\Omega_{g-1, g}$ is the gap between consecutive gray levels and it is measured with the help of rank vector, as

$$\Omega_{g-1, g} = (r(g-1) + r(g))/2 \quad (13)$$

This gap is calculated based on the joint contribution of successive gray levels. The gap specified in above expression is nothing but the average of ranks of two successive gray levels. Importantly, if any output gray value is not an integer, then it was rounded to its nearest integer. This method ensured guaranteed utilization of allowed dynamic range b_l and b_u as they are minimum and maximum ranges respectively. The complete utilization and the consideration of mutual relationship between gray levels ensure an increased contrast in the output image.

4. Experimental results

4.1 Testing dataset


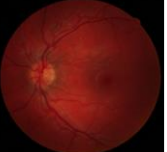
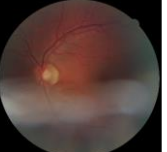
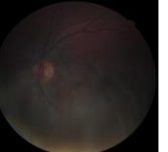
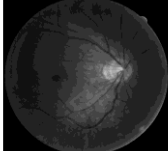
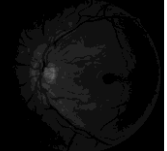
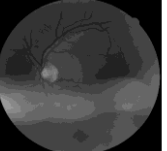
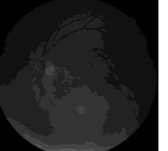
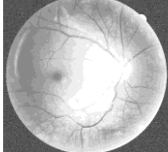
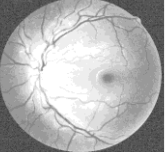

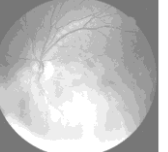
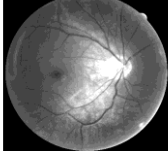
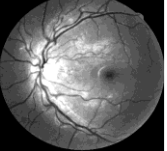
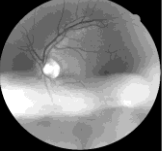
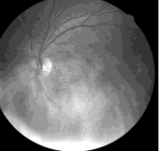
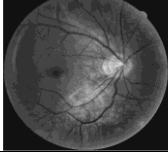
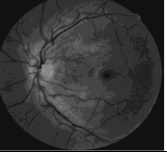
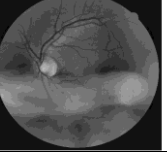
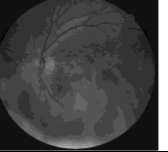

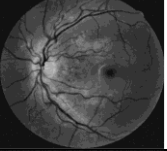
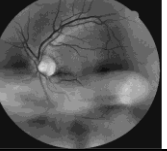
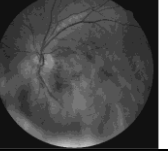
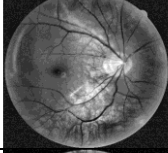
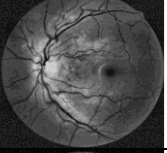

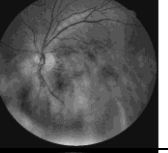
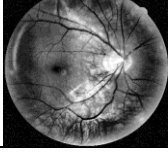
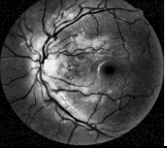
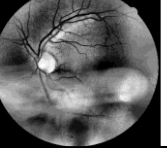

To validate the proposed method, it was tested over different retinal images that were collected from different datasets. This work is employed totally on two standard datasets namely High Resolution Fundus (HRF) [31] database and DRIVE database [32]. HRF is captured with the help of 18 human subjects using a Canon CR-1 fundus camera.

For all the subjects they captured the 18 pairs of same eyes and they kept the camera at the field of View of 45° . For every pair, the initial image is captured with less quality and second image is captured with more quality. At this simulation phase, we consider only poor quality images [33]. Next, DRIVE dataset consists of totally 40 color fundus images with .JPEG format. They were acquired through a Canon CR5 non-mydratic 3CCD fundus camera at FOV of 45° . All the images are captured from Netherlands through a DR screening program. The resolution of each image is 584×565 pixels, 8-bit version and each one composed of three (Red, Green and Blue) channels. The entire 40 images are segmented as training and testing images. For our simulation, we employed all the 40 images.

For the comparison purpose, we considered some earlier methods and some recent methods whose main objective is to enhance the quality of retinal images. In the category of earlier methods, we considered the most popular HE [8] and CLAHE [14]. Some authors referred CLAHE as a base method and they extended it by applying some filters before processing the image through CLAHE. Among such kind of methods, the recent method Filtered CLAHE (FCLAHE) [25] applied different filters and Transformed CLAHE (TCLAHE) [27] applied curvelet transform. Different from these methods, Normalized Convolution (NC) [20] used PDEs and RMF for contrast enhancement. For a fair comparison, we referred all kinds of methods and the result obtained through these methods and proposed method (SCCE) is shown below;

Table.1 and Table.2 show the results of HRF and DRIVE databases respectively. These results explore the visual quality of retinal images and it can be observed visually. From these results, we can observe that the output image of proposed SCCE is better than all the other existing methods. This observation can be done in both case studies. Thus, the proposed method can be regarded as a better approach for contrast enhancement even for the images of poor quality. To alleviate the effectiveness of proposed method, we referred these two datasets among which one is composed of poor quality image and another one of better quality images. The obtained visual results reveal that the proposed SCCE can preserve the contrast quality of retinal images in any circumstances. Compared to the output images obtained through existing methods, the vessel structure is clearer in the output images obtained through SCCE. This is the main requirement for any vessel segmentation method and hence the proposed method can be used as a

Table 1. Original and contrast enhanced retinal images of HRF database evaluated through different methods

Method/Image				
Green Channel				
HE [8]				
CLAHE [14]				
FCLAHE [25]				
TCLAHE [27]				
NC [20]				
SCCE				

successful pre-processing method in the system for DR diagnosis.

4.2 Performance metrics

To further explore the performance effectiveness of SCCE, the obtained visual results (output images) are subjected to quantitative evaluation and under this evaluation, several performance metrics are measured. Totally, we consider two metrics namely Structural Similarity Index Measure (SSIM), Contrast Improvement Index (CII) [34] and Linear Index of Fuzziness (LIF) [35]. CII measures the improvement in the contrast from original image to contrast enhanced image. CII is calculated with the





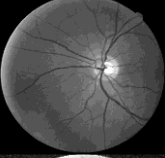
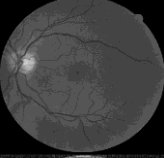
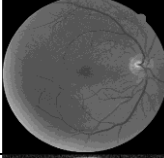
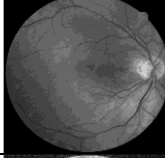
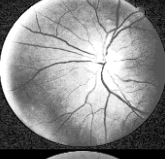
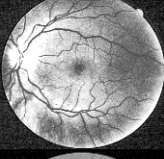
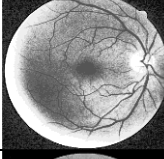
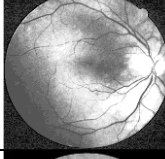



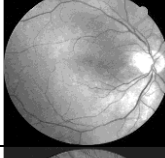



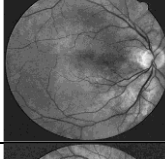
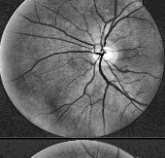

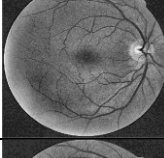
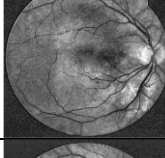
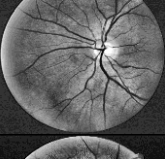

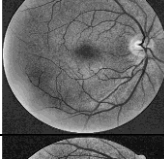
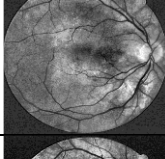
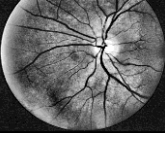
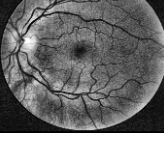
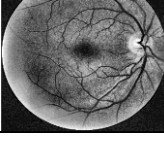
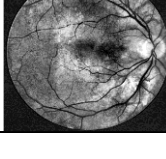
help of two measures namely contrast of original image (C) and contrast of enhanced image (C_e). With the help of C and C_e , the CII is formulated as

$$CII = \frac{C_e}{C} \tag{14}$$

Where C is initially measured with the help of the objects and background of original input image. In the retinal image, the objects are nothing but retinal vessels. Mathematically the C is computed as follows;

$$C = \frac{|Y-G|}{|Y+G|} \tag{15}$$

Table 2. Original and contrast enhanced retinal images of DRIVE database evaluated through different methods

Method/Image				
Green Channel				
HE [8]				
CLAHE [14]				
FCLAHE [25]				
TCLAHE [27]				
NC [20]				
SCCE				

Where Y and G are the gray values of vessels and non-veessels respectively. Based on the above expression, we can understand that a larger value of C denotes a larger gap between vessels and non-vessel region (background region). C_e is also measured in the same manner and a larger value of C_e indicates better performance. As the vlaue of C_e is high, the CII is also high and it denotes a better contrast enhancement in the resultant image. The next meausre is LIF which is a one of quantitative meausre used for the analysis of quality improvement in images. Mathematcally the LIF is measuerd as

$$\gamma(I) = \frac{2}{M \times N} \sum_{m=1}^M \sum_{n=1}^N \min\{p(m, n), (1 - p(m, n))\} \quad (16)$$

Where

$$p(m, n) = \sin \left[\frac{\pi}{2} \times 1 - \left(\frac{I(m, n)}{I_{max}} \right) \right] \quad (17)$$

Where $I(m, n)$ denotes the gray value of the pixel at (m,n), I_{max} is the maximum gray level of image I of size $M \times N$. As the value of γ is small, the method is said to have better performance and the resultant images have better quality.

Next, SSIM explores the structural similarity between original and enhanced image. In this work, the original image is reflected by input low contrast

image and output image is reflected by the contrast enhanced image. The SSIM is measured between them to find the deviations in the structure of image. Since the main objective of proposed method is to enhance only the contrast, the structural features must remain same. Hence, SSIM is considered here for the assessment of performance of proposed contrast enhancement method. The mathematical expression for SSIM is given as

$$SSIM = \frac{(2 \times \bar{x} \times \bar{y} + C_1)(2 \times \sigma_{xy} \times C_2)}{(\sigma_x^2 + \sigma_y^2 + C_1)(\bar{x}^2 + \bar{y}^2 + C_2)} \quad (18)$$

Where $C_1 = (k_1 L)^2$ and $C_2 = (k_2 L)^2$ those avoids the fraction from infinity. L is the dynamic range of the pixel values (typically this is 2# bits per pixel -1). $k_1 = 0.01$ and $k_2 = 0.03$ by default. The default range of SSIM lies in between -1 and 1. Hence, the SSIM and CII value must be high and LIF value must be low to indicate the good performance. The following Table.3 and Table.4 shows the CII and LIF values of HRF and DRIVE databases respectively.

Table 3 and Table 4 shows the comparison of CII and LIF between proposed and several existing

methods through HRF images and DRIVE images respectively. From the values, we can observe that the proposed method has larger CII and smaller LIF for all test images. Among the existing methods, the HE is observed to have much lesser performance because it produces an uneven retinal image which changes the illumination of background. This kind of artifact is termed as over enhancement and due to this issue, the objects such as retinal vessels and non-vessels seem to have similar illumination. However, this is not a vital solution and it consequences to a serious degradation in performance during vessel segmentation. Next, CLAHE is a better method for CE and shows an effective performance compared to HE. However, the CLAHE needs an additional parameter setting and they are different for different regions. A clip limit is set for one region won't produce better results for other regions. The clip limit for smoother contrast region seeks lower value but for edge region, it is not a better solution. We can observe that for all images, the CII value of CLAHE has jumped very long from HE while the further CLAHE based methods such as FCLAHE and

Table 3. CII and LIF comparison of HRF database images

Image	Metric	HE	CLAHE	FCLAHE [25]	TCLAHE [27]	NC [20]	SCCE
Image 1	CII	1.0012	1.9645	2.2145	2.3381	3.0074	4.5441
	LIF	0.5574	0.8421	0.5014	0.4971	0.5111	0.4586
	SSIM	0.4929	0.6854	0.7254	0.7586	0.8224	0.8779
Image 2	CII	1.5842	2.3315	2.8647	2.5897	3.3333	3.9647
	LIF	0.7888	0.8542	0.6342	0.6014	0.5638	0.5047
	SSIM	0.3817	0.5234	0.5638	0.5966	0.6874	0.7586
Image 3	CII	1.1282	2.0915	2.3145	2.4651	3.1344	4.6711
	LIF	0.6844	0.9691	0.6284	0.6241	0.6381	0.5853
	SSIM	0.5364	0.7332	0.7584	0.7999	0.8564	0.9196
Image 4	CII	1.6817	2.4290	2.9622	2.6872	3.4308	4.0622
	LIF	0.8863	0.9517	0.7317	0.6989	0.6613	0.6022
	SSIM	0.3923	0.5924	0.6124	0.6541	0.7014	0.8114

Table 4. CII and LIF comparison of DRIVE database images

Image	Metric	HE	CLAHE	FCLAHE [25]	TCLAHE [27]	NC [20]	SCCE
Image 1	CII	2.2441	3.0651	3.5689	3.8645	4.9967	6.3478
	LIF	0.5193	0.6642	0.6401	0.6037	0.4721	0.3324
	SSIM	0.5148	0.7741	0.7964	0.8145	0.8694	0.9035
Image 2	CII	1.4042	3.6009	3.6245	3.6689	4.8542	6.3314
	SSIM	0.5306	0.7411	0.7638	0.7984	0.8333	0.9014
	LIF	0.6024	0.5441	0.5214	0.5475	0.5023	0.4012
Image 3	CII	2.2314	2.9362	3.2145	3.4478	4.5662	5.8978
	LIF	0.5527	0.4523	0.4875	0.4663	0.4112	0.3669
	SSIM	0.7555	0.8366	0.8666	0.8964	0.9147	0.9478
Image 4	CII	2.9720	2.9169	3.4478	3.8975	5.6348	7.8894
	LIF	0.4865	0.3354	0.3865	0.3559	0.3045	0.2547
	SSIM	0.5968	0.6978	0.7148	0.7444	0.7996	0.8638

TCLAHE has only a smaller jump. Since these two methods adapted CLAHE as a base method and applied different filters before CLAHE, they have gained a slight improvement than the CLAHE. FCLAHE applied various filter such as median filter, wiener filter, Gaussian filter etc., as a noise removal filters before processing the retinal images for contrast enhancement. These filters won't have much contribution in contrast enhancement and illumination adjustment as they are much better in the removal of noises. Hence FCLAHE has a gained slight improvement. Similarly, TCLAHE also adapted CLAHE as a base method and decomposed the image into sub bands through curvelet before processing it for CE. The sub bands explore the local features of retinal image which don't have much contribution on the global contrast enhancement. From the observed values, it can be noticed that FCAHE also gained a slight improvement in CE than CLAHE. Next, TCLAHE employed PDEs and RMF as a normalized convolution to enhance the contrast in retinal images. Even though it has gained a superior performance compared to HE and CLAHE, intensity distribution is uniform it doesn't consider the spatial mutual relation between gray levels hence the gap between consecutive gray levels is low. This problem makes the image to look like a burning image whose background of retinal vessels also looks enhanced. Finally, the proposed SCCE is observed to have a better performance compared to existing methods. The proposed method shows some merits compared to other methods. They are (1) the vessel edges varies much softly as they are spurious and abrupt changes in the image that consist of basic information. (2) Spatial collaboration between adjacent gray levels provides a perfect discrimination between vessel pixels and non-vessel pixels thereby the contrast at vessels and non-vessels is enhanced perfectly.

Fig. 2 shows the comparison between proposed and existing methods through the CII value obtained after the simulation of images of HRF database. From this figure, the average CII of Histogram equalization method is observed as 1.4257, for CLAHE it is observed as 2.5672, for FCLAHE, TCLAHE and NC, it is observed as 2.6035, 2.6988, and 3.3386 respectively. Finally, for the proposed method, the average CII is noticed as 4.3927 which is larger value than the existing methods.

Fig. 3 shows the comparison between proposed and existing methods through the CII value obtained after the simulation of images of DRIVE database. From this figure, the average CII of Histogram equalization method is observed as 2.0821, for

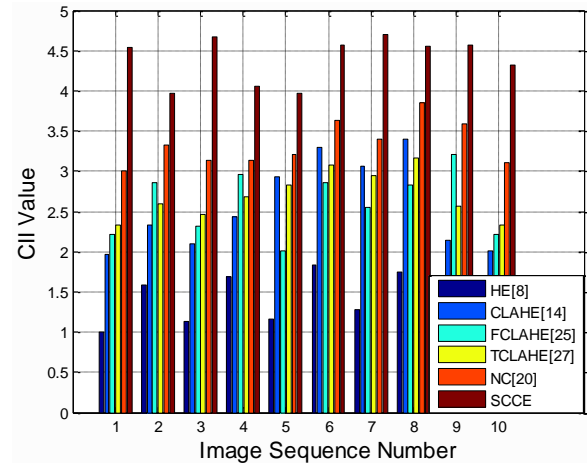


Figure. 2 Comparison of CII for different images of HRF database

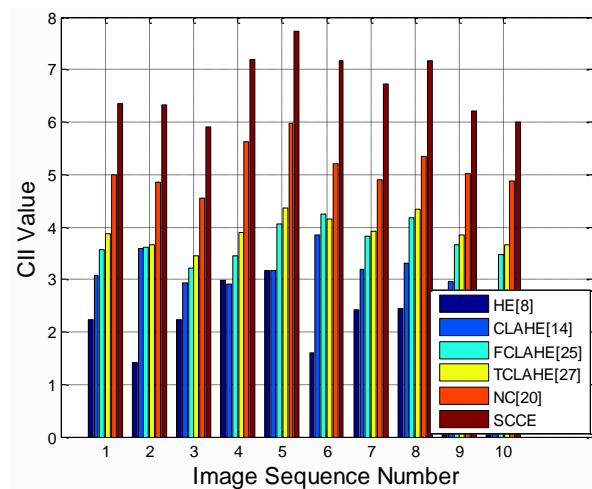


Figure. 3 Comparison of CII for different images of DRIVE database

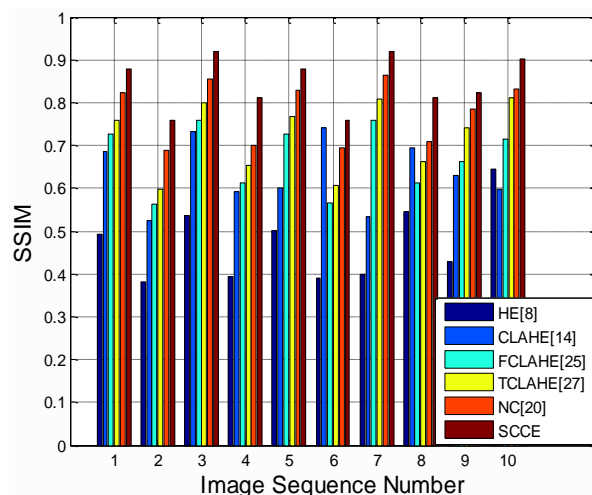


Figure. 4 Comparison of SSIM for different images of HRF database

CLAHE it is observed as 2.8988, for FCLAHE, TCLAHE and NC, it is observed as 3.3844, 3.5497, and 4.6497 respectively. Finally, for the proposed

method, the average CII is noticed as 6.0771 which is of larger value than the existing methods. From these values, it can be noticed that the CII of DRIVE database is larger than the HRF database. The main reason is that the DRIVE images are of good quality while the HRF images are of bad quality. Thus, we can state that the proposed method performs well not only for good quality images but also for bad quality images.

Next, Fig. 4 shows the comparison between proposed and earlier methods though SSIM performance metric. The larger value of SSIM reflects better structural preservation. As it approaches to 1, the method is said to perform well in the preservation of structural features. From the Table 3, it can be noticed that the proposed SCCE had gained a larger value of SSIM for all input images. Moreover, it can also be noticed that the SCCE had shown its superior performance even in the case of low resolution images, i.e., HRF images. The average SSIM of earlier methods is measured as 0.4713, 0.6334, 0.6703, 0.7209, and 0.7779 for HE, CLAHE, FLCAHE, TCLAHE and NC respectively. The proposed SCCE had shown its superiority by obtaining the maximum SSIM (0.8466) which is a very much larger value than the SSIMs of conventional methods.

5. Conclusion

In this paper, a new method is introduced for contrast enhancement in retinal images. This method introduced a new definition for mutual dependency calculation between consecutive gray levels thereby the gap is more and results in an improved contrast. The proposed spatial collaboration between gray levels controls the contrast level without any need of additional parameter setting like CLAHE and its subsequent methods. Extensive quantitative and qualitative experiments prove that the proposed method can improve the contrast to an appropriate level such that the objects in retinal images are clearly distinguishable. To prove the robustness, different types of images are processed and the performance is assessed quantitatively. This achievement makes the proposed approach applicable for contrast enhancement in retinal images for all environments. From the results, it has been observed that the SCCE has gained an improvement in the CII is of 6.57%, 5.23%, 4.43%, 4.13% and 2.31% from HE, CLAHE, FLCAHE, TCLAHE and NC respectively. As well as the SSIM improvement is observed as 4.43%, 2.51%, 2.08%, 1.48% and 1.15% from HE, CLAHE, FLCAHE, TCLAHE and NC respectively.

References

- [1] N. Congdon, Y. Zheng, and M. He, "The worldwide epidemic of diabetic retinopathy", *Indian J. Ophthalmol.*, Vol. 60, No. 5, pp. 428-431, 2012.
- [2] J. W. Y. Yau, S. L. Rogers, R. Kawasaki, E. L. Lamoureux, J. W. Kowalski, T. Bek, S. J. Chen, J. M. Dekker, A. Fletcher, J. Grauslund, S. Haffner, R. F. Hamman, M. K. Ikram, T. Kayama, B. E. K. Klein, R. Klein, S. Krishnaiah, K. Mayurasakorn, J. P. O'Hare, T. J. Orchard, M. Porta, M. Rema, M. S. Roy, T. Sharma, J. Shaw, H. Taylor, J. M. Tielsch, R. Varma, J. J. Wang, N. Wang, S. West, L. Xu, M. Yasuda, X. Zhang, P. Mitchell, and T. Y. Wong, "Global prevalence and major risk factors of diabetic retinopathy", *Diab. Care*, Vol. 35, No. 3, pp. 556-564, 2012.
- [3] M. M. Nentwich and M. W. Ulbig, "Diabetic retinopathy - ocular complications of diabetes mellitus", *World J. Diab.*, Vol. 6, No. 3, pp. 489-499, 2015.
- [4] G. D. Joshi and J. Sivaswamy, "Colour retinal image enhancement based on domain knowledge", In: *Proc. of International Conf. on Computer Vision, Graphics & Image Processing*, pp. 591-598, 2008.
- [5] A. A. Youssif, A. Z. Ghalwash, and A. S. Ghoneim, "Comparative study of contrast enhancement and illumination equalization methods for retinal vasculature segmentation", In: *Proc. of International Conf. on Biomedical Engineering*, pp. 1-5, 2006.
- [6] A. A. Youssif, A. Z. Ghalwash, and A. S. Ghoneim, "A comparative evaluation of preprocessing methods for automatic detection of retinal anatomy", In: *Proc. of International Conf. on Informatics and Systems*, pp. 24-30, 2007.
- [7] A. K. Nandi and N. M. Salem, "Novel and adaptive contribution of the red channel in pre-processing of colour fundus images", *J. Franklin Inst.*, Vol. 344, No. 3, pp. 243-256, 2007.
- [8] Y. Zheng, F. Coenen, and M. H. A. Hijazi, "Retinal image classification is using a histogram based approach", In: *Proc. of International Joint Conf. on Neural Networks*, pp. 1-7, 2010.
- [9] W. L. Yun, U. R. Acharya, Y. V. Venkatesh, C. Chee, L. C. Min, and E. Y. K. Ng, "Identification of different stages of diabetic retinopathy using retinal optical images", *Inf. Sci.*, Vol. 178, No. 1, pp. 106-121, 2008.

- [10] T. Sund and A. Møystad, "Sliding window adaptive histogram equalization of intra-oral radiographs: effect on diagnostic quality", *Dentomaxillofac Radiol.*, Vol. 35, No. 3, pp. 133-138, 2006.
- [11] S. R. Krishnai and S. K. Shome, "Enhancement of Diabetic Retinopathy Imagery Using Contrast Limited Adaptive Histogram Equalization", *International Journal of Computer Science and Information Technologies*, Vol. 2, No. 6, pp. 2694-2699, 2011.
- [12] A. B. Suksmono, O. S. Santosa, T. R. Mengko, and A. W. Setiawan, "Color Retinal Image Enhancement using CLAHE", In: *Proc. of International Conference on ICT for Smart Society*, pp. 1-3, 2013.
- [13] H. Rahim, A. S. Ibrahim, W. M. Diyana, and A. Hussain, "Methods to Enhance Digital Fundus Image for Diabetic Retinopathy Detection", In: *Proc. of International Colloquium on Signal Processing & its Applications*, pp. 221-225, 2014.
- [14] T. Jintasuttisak and S. Intajag, "Color Retinal Image Enhancement by Rayleigh Contrast-Limited Adaptive Histogram Equalization", In: *Proc. of International Conf. on Control, Automation and Systems*, pp. 22-25, 2014.
- [15] T. P. Das, B. Ramanathan, R. K. Kumar, and H. Rampal, "Complex shock filtering applied to retinal image enhancement", In: *Proc. of World Congress on Medical Physics and Biomedical Engineering*, pp. 900-903, 2012.
- [16] G. Gilboa, N. Sochen, and Y. Y. Zeevi, "Image Enhancement and denoising by complex diffusion process", *IEEE Trans. Pattern Anal. Mach. Intell.*, Vol. 26, No. 8, pp. 1020-1036, 2004.
- [17] P. S. Dai, X. H. Wang, Y. Q. Zhao, and M. Liao, "Retinal vessel enhancement based on multi-scale top-hat transformation and histogram fitting stretching", *Optics and Laser Technology*, Vol. 58, No. 6, pp. 56-62, 2014.
- [18] X. Bai, F. Zhou, and B. Xue, "Image enhancement using multi-scale image features extracted by top-hat transform", *Opt. Laser Technol.* Vol. 44, No. 2, pp. 328-336, 2012.
- [19] L. Yang, Y. Liang, and H. Fan, "Study on the methods of image enhancement for liver CT images", *Optik*, Vol. 121, No. 19, pp. 1752-1755, 2010.
- [20] M. Fan, P. Dai, H. Sheng, and J. Zhang, "Retinal Fundus Image Enhancement Using the Normalized Convolution and Noise Removing", *International Journal of Biomedical Imaging*, Vol. 2016, pp. 1-12, 2016.
- [21] H. Knutsson and C. F. Westin, "Normalized and differential convolution methods for interpolation and filtering of incomplete and uncertain data", In: *Proc. of the IEEE Conference on Computer Vision and Pattern Recognition*, pp. 515-523, 1993.
- [22] L. Luo, T. Tong, Z. Shao, Y. Chen, and B. Chen, "Blood Vessel enhancement via multi-dictionary and sparse coding: Application to retinal vessel enhancing", *Neurocomputing*, Vol. 200, No. 5, pp. 110-117, 2016.
- [23] X. Liang and L. Xiong, "An Enhancement Method for Color Retinal Images Based on Image Formation Model", *Comput Methods Programs Biomed.*, Vol. 143, No. 3, pp. 137-150, 2017.
- [24] M. Zhou, K. Jin, S. Wang, J. Ye, and D. Qian, "Color retinal image enhancement based on luminosity and contrast adjustment", *IEEE Trans. Biomed. Eng.*, Vol. 65, No. 3, pp. 521-527, 2018.
- [25] S. S. Sonali, A. K. Singh, S. P. Gherera, and M. Elhonseny, "An approach for de-noising and contrast enhancement of retinal fundus image using CLAHE", *Optics & Laser Technology*, Vol. 110, pp. 87-98, 2019.
- [26] B. Gupta and M. Tiwari, "Color Retinal image Enhancement using luminosity and Quantile based contrast enhancement", *Multiidim Syst Sign Process*, Vol. 30, pp. 1829-1837, 2019.
- [27] A. A. Bala, P. A. Priya, and V. Maik, "Retinal Image Enhancement Using Curvelet Based Sigmoid Mapping of Histogram Equalization", *Journal of Physics: Conference Series*, Vol. 1964, pp. 1-9, 2021.
- [28] T. Celik, "Spatial Entropy-Based Global and Local Image Contrast Enhancement", *IEEE Transactions on Image Processing*, Vol. 23, No. 12, pp. 5298-5308, 2014.
- [29] T. Celik and H. C. Li, "Residual spatial entropy-based contrast enhancement and gradient-based contrast measures", *Journal of Modern Optics*, Vol. 63, No. 16, pp. 1600-1617, 2016.
- [30] P. Berkhin, "A survey on page rank computing", *Internet Mathematics*, Vol. 2, No. 1, pp. 73-120, 2005.
- [31] A. Budai, R. Bock, A. Maier, J. Hornegger, and G. Michelson, "Robust Vessel Segmentation in Fundus Images", *International Journal of Biomedical Imaging*, Vol. 2013, No. 6, pp. 1-11, 2013.

- [32] J. Staal, M. D. Abr`amoff, M. Niemeijer, M. A. Viergever, and B. V. Ginneken, "Ridge-based vessel segmentation in color images of the retina", *IEEE Transactions on Medical Imaging*, Vol. 23, No. 4, pp. 501-509, 2004.
- [33] K. Thomas, A. Budai, K. Martin, J. Odstrcilik, G. Michelson, and J. Hornegger, "Automatic No-Reference Quality Assessment for Retinal Fundus Images Using Vessel Segmentation", In: *Proc. of International Symposium on Computer-Based Medical Systems*, pp. 95-101, 2013.
- [34] J. Oh and H. Hwang, "Feature enhancement of medical images using morphology-based homomorphic filter and differential evolution algorithm", *International Journal of Control, Automation and Systems*, Vol. 8, No. 4, pp. 857-861, 2010
- [35] X. Z. Bai, F. G. Zhou, and B. D. Xue, "Image enhancement using multi scale image features extracted by top-hat transform", *Optics and Laser Technology*, Vol. 44, No. 2, pp. 328-336, 2012.